JOURNAL OF MECHANICAL ENGINEERING AND SCIENCES
ISSN: 2289-4659 e-ISSN: 2231-8380
VOLUME 20, ISSUE 1, 2026, 11095 - 11107
DOI: https://doi.org/10.15282/jmes.20.1.2026.6.0866

RESEARCH ARTICLE

The effect of adding *Casuarina equisetifolia* fruit powder on the wear, impact strength, and hardness of motorcycle disc brake pad composites

Nurin Tammima, Heri Yudiono*, Muhammad Irfan Rifaldi

Department of Mechanical Engineering, Faculty of Engineering, Universitas Negeri Semarang, Semarang 50229, Central Java, Indonesia

Abstract - Natural fiber composites are widely studied as an alternative in engineering, especially for tribological applications such as brake pads in the automotive industry. This study analyzes the effect of *Casuarina equisetifolia* fruit powder on wear, impact strength, and hardness of epoxy matrix brake pads. The research used a true experimental design with a posttest-only control group. The results showed that the 30% CEFP composite was almost equivalent to the control group, with a specific wear value of 8.33×10^{-4} $mm^3/kg \cdot m$, having a difference of 28.93% from commercial products, an average impact strength value of 2.08×10^{-3} J/mm^2, a difference of 20.19%, and an average hardness value of 13.4 HV, a difference of 36.04%, which shows potential for low-load automotive applications.

Article History
Received : 30 August 2025
Revised : 25 February 2026
Accepted : 16 March 2026
Published : 31 March 2026

Keywords
Composite materials
Brake pads
Casuarina equisetifolia fruit
Specific wear rate
Impact strength
Hardness

1. Introduction

Brake pads are an important component in motor vehicles that are susceptible to harsh tribological conditions. Choosing the right brake pad material is very important [1]. Natural fibers are being investigated as potential replacements for synthetic fibers in fiber-reinforced composites. The advantages of natural fibers are low density, low cost, high flexural modulus, high impact strength, specific properties, renewability, non-corrosiveness, and ease of production. Due to their biodegradability, natural fibers are widely used across sectors such as transportation, aerospace, and automotive. In addition, the research also includes the manufacture of composites with thermoplastic polymers and reinforcing fillers made from recycled waste, especially lignocellulose materials [2-3]. The fruit of *Casuarina equisetifolia* is a natural material that has a fairly high content of lignocellulose. Due to its considerable existence, waste from this fruit is often used as a source of activated carbon because it has a high carbon content [4]. *Casuarina equisetifolia* has round, wide, and stiff fruits resembling pine fruits, as shown. The fruit is encased in a wooden structure measuring 0.75 in (2 cm) long and resembling a cone. Mature fruits are brownish-red or gray [5]. The lignocellulose content of the *Casuarina equisetifolia* fruit makes it suitable for use as a filler in composites. In addition to fillers, composite materials have a matrix structure. The matrix widely used in composite manufacturing is epoxy resin. This is due to its thermal, mechanical, and electrical properties, as well as its dimensional stability and chemical resistance [6]. In the manufacture of natural fiber-reinforced brake pad composites, the addition of aluminum oxide powder can improve the composite's flexural and impact strength [7].

These materials have many advantages. Therefore, further research is needed to explore the potential of natural fibers as an alternative material for brake pad composites. Because each natural material has unique potential. By taking advantage of this, we can create a new formula that is environmentally friendly and sustainable. In addition, using natural materials as composite materials for brake pads can help overcome the problem of organic waste accumulation. There is a substantial research gap in the use of *Casuarina equisetifolia* fruit waste as friction materials. While numerous natural fillers have been explored, CEFP's high lignin content (46.06%) and carbon yield confer functional advantages, including thermal stability and structural rigidity, both of which are required in automotive braking systems. This study provides a preliminary investigation of mechanical properties to address the limitations of current waste-based composites, which often lack adequate wear resistance. While this study focuses on fundamental mechanical properties (wear, impact, and hardness), it is acknowledged that a full friction material characterization requires future testing of friction coefficient stability, fade resistance, and thermal conductivity to determine complete commercial viability. This research is expected to support innovation in materials technology and the sustainable manufacturing sector by contributing to the development of brake pad composite materials with more reliable mechanical performance. This aligns with Sustainable Development Goals (SDG 9: Industry, Innovation, and Infrastructure).

2. Methods and Materials

2.1 *Casuarina equisetifolia* Fruit

Casuarina equisetifolia fruit waste was collected from Lombang Beach, Sumenep Regency, East Java, Indonesia. The fruit was then dried under the hot sun until it turned reddish brown and did not release liquid when broken (± 7 days). After drying, the fruit was ground in a chopper. Then, the powder was sieved using a 100-mesh sieve. The visual appearance of the prepared Casuarina equisetifolia fruit powder is shown in Figure 1. A density test was conducted to determine its specific gravity. To better understand the material's properties and suitability as a composite filler, the proximate, ultimate, and biochemical analysis of the Casuarina equisetifolia fruit waste is presented in Table 1 [8].

***CORRESPONDING AUTHOR | Heri Yudiono** | ✉ heri_yudiono@mail.unnes.ac.id

Table 1. Proximate, ultimate, and biochemical analysis of Casuarina equisetifolia fruit waste [8]

Parameters		*Casuarina equisetifolia* fruit waste (wt%) in dry conditions
Proximate analysis	Moisture	1.20 ± 0.32
	Ash	2.65 ± 0.51
	Volatile matter	75.81 ± 0.4
	Fixed carbon	19.38 ± 0.21
Ultimate analysis	Carbon	43.87
	Hydrogen	5.34
	Nitrogen	1.61
	Sulfur	0.11
	Oxygen	49.07
Biochemical analysis	Cellulose	25.52 ± 0.01
	Hemicellulose	18.84 ± 0.01
	Lignin	46.06 ± 0.01

Figure 1. *Casuarina equisetifolia* fruit powder

2.2 Aluminium Oxide Powder

Alumina, or aluminum oxide (Al_2O_3), is a white, amorphous powder that is amphoteric and extremely stable. In nature, alumina can also be found as the mineral corundum. represents an extremely hard substance that is used as a polishing and grinding abrasive [9]. Aluminum oxide powder was obtained from a chemical supply store in Semarang. The powder size is 100 mesh. The detailed physical and mechanical properties of the aluminum oxide are presented in Table 2 [9]. The visual appearance of the aluminium oxide powder used in this study is shown in Figure 2.

Table 2. Physical and mechanical properties of aluminum oxide [9]

Characteristic	Value
Physical state	Solid
Colour	White
Molar mass (g/mol)	101.96
Density (g/cm^3)	3.95
Melting point (°C)	2072
Boiling point (°C)	2977
Hardness (kgf/mm^2)	1500-1800
Thermal conductivity (W/m.K)	20-30
Strength (compressive) (MPa)	2000-4000
Strength (mechanical) (MPa)	300-630
Electrical resistivity (Ωm)	10^{12}-10^{13}

Figure 2. Aluminium oxide powder

2.3 Epoxy Resin

Bisphenol A-Epichlorohydrin type epoxy resin, and Cycloaliphatic Amine type hardener are used as the matrix. Epoxy resin has several advantages, including high-temperature resistance and excellent adhesion. Binders play a crucial role in friction materials, keeping everything together and withstanding high temperatures and pressures [10]. The specific physical and mechanical properties of the epoxy resin used as the matrix are detailed in Table 3 [11]. The packaging and visual appearance of the epoxy resin and hardener are shown in Figure 3.

Table 3. Physical and mechanical properties of epoxy resin [11]

Properties	Value
Elongation at break (%)	5
Heat distortion temperature (°C)	120
Tensile strength (MPa)	~85
Density (g/cm^3)	1.11-1.23
Compressive strength (MPa)	~11
Tensile elastic modulus (GPa)	~3.2
Flexural strength (MPa)	~130
Linear expansion coefficient (in 10^{-6}/°C)	60
Water absorption/24 h (%)	0.14
Rockwell hardness/6.23 mm, 100 kg (Rockwell)	100
Shrinkage rate (%)	1-2

Figure 3. Epoxy resin

2.4 Methods

This study uses an experimental method. This method is used to determine the cause-and-effect relationship between variables intentionally manipulated by the researcher. The design used is a true experimental design, a posttest-only control design. The experimental group is a composite specimen prepared with a composition of *Casuarina equisetifolia* fruit powder (CEFP), aluminum oxide powder, epoxy, and hardener. The composition is varied into three. Meanwhile, the front disc brake pads for a motorcycle with code 06455-KYE-901 are used as the control group. The brake pads are Honda-branded. They can be used by motorcycles Mega Pro New, Verza 150, CB150 Verza, CB150R StreetFire K15G, and CB150R StreetFire K15M. In this study, Honda brake pads were used only as a reference. Commercial brake pads typically use complex multi-component systems that include binders, lubricants, and friction modifiers. Meanwhile, this study used a simplified ternary formulation (CEFP, Al_2O_3, and epoxy) to isolate the mechanical effects of natural fillers.

This simplified model provides a basis for evaluating the functional feasibility of CEFP in a polymer matrix. The specific mass and weight percentages for each of the three composition variations are detailed in Table 4.

Table 4. Composite formula

No	CEFP	Al_2O_3	Epoxy
1	10% (8.85 g)	20% (48.6 g)	70% (85.05 g)
2	20% (17.69 g)	20% (48.6 g)	60% (72.9 g)
3	30% (26.54 g)	20% (48.6 g)	50% (60.75 g)

2.5 Composite Preparation

The equipment used includes chopper machines, 100 mesh sieves, digital scales, mixers, specimen moulds, press machines, callipers, bevel protractors, sandpaper, brushes, hand grinders, hot guns, ovens, microscope type B-510 METROPTIKA ITALY, Ogoshi High Speed Universal Wear Testing Machine (Type OAT-U), Gotech Impact Testing Machine, and Microhardness Tester Fm-800. Meanwhile, the materials used include *Casuarina equisetifolia* fruit powder, aluminum oxide powder, epoxy resin, and hardener. The composite manufacturing process begins with preparing tools and materials. *Casuarina equisetifolia* fruit is dried under the hot sun until it turns reddish brown and does not release liquid when broken (± 7 days). After drying, the fruit is ground in a grinder. Then, the powder is sieved through a 100-mesh sieve. A density test is carried out to determine the specific gravity of *Casuarina equisetifolia* fruit powder, aluminum oxide powder, epoxy resin, and hardener. Next, the volume fraction is calculated to determine the composition of each material. The epoxy resin and hardener are mixed in a 1:1 ratio. Then, both powders are mixed with epoxy resin and hardener using a dry mixing technique.

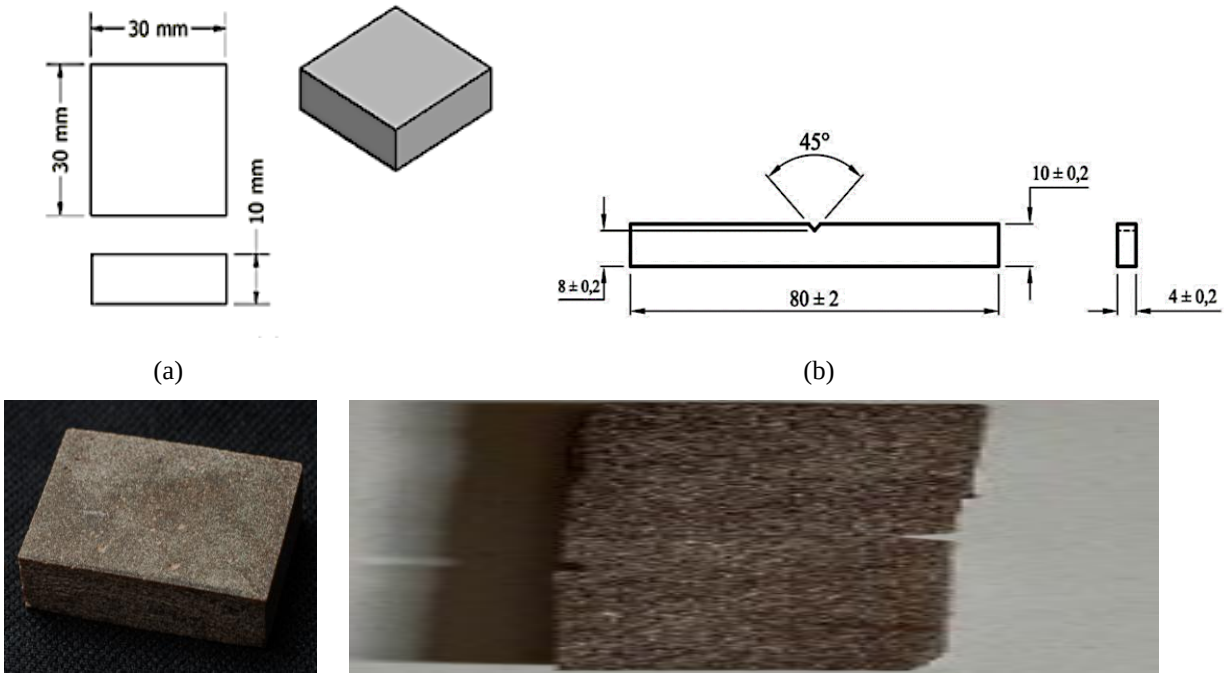

Figure 4. Dimensions and physical appearances of the experimental test specimens: (a) schematic dimensions for the Ogoshi wear and hardness tests, (b) schematic dimensions for the Charpy impact test, (c) fabricated specimen for the Ogoshi wear and hardness tests, and (d) fabricated specimen for the Charpy impact test

The mixed ingredients are then poured into moulds and pressed. The pressure applied is 1,500 psi for 10 minutes. The pressing process is carried out using a one-way hydraulic press using the cold compression method [12]. After the composite is moulded, the next stage is the post-curing process using an oven. The composite is ovened at 108 °C for 30 minutes [13]. The post-curing temperature of 108 °C was selected to ensure maximum cross-linking of the Cycloaliphatic Amine hardener without exceeding the resin's Heat Distortion Temperature (120 °C). Next, the composite is cut according to the applicable size standards. The specific wear test specimen size is based on the Ogoshi High-Speed Universal Wear Testing Machine (OAT-U Type) from Gadjah Mada University. The Charpy impact test specimen size is specified in ISO 179-1 [14]. The schematic dimensions and the physical appearance of the fabricated test specimens are illustrated in Figure 4. Each composition variation was made into three specimens for wear and impact testing.

2.6 Specific Wear Rate

The specific wear test in this study uses the Ogoshi method. This is done to determine the wear rate of a material by measuring the width of the wear trace on the material resulting from friction with a rotating disc. The test was conducted

at the Engineering Materials Laboratory, Department of Mechanical and Industrial Engineering, Gadjah Mada University, Yogyakarta, using the Ogoshi High Speed Universal Wear Testing Machine (Type OAT-U). Each variation was made on as many as three test specimens to ensure the statistical reliability of the results. The results of this test are the wear width of the test specimen. The data obtained are then entered into Eq. (1) to calculate the specific wear rate.

$$W_s = \frac{B \times b_0^3}{8r \times p_0 \times l_0} \quad (1)$$

where, B is the width of revolving disc (mm), b_0 is width of wear on the test object (mm), r is the radius of revolving disc (mm), $p_0$is the compressive force during the wear process (kg), l_0 is distance traveled in the wear process (m), W_s is specific wear rate (mm^3/kgm).

2.7 Impact Strength Test

The impact test in this study used the Charpy method. The aim is to measure a material's ability to absorb energy due to shock loads. The test was conducted at the Mechanical Engineering Materials Testing Laboratory, Faculty of Engineering, Semarang State University, using a Gotech brand impact tester. Each variation was tested on up to three test specimens to ensure data consistency. The results obtained from this test are the absorbed energy value. The data obtained are then entered into Eq. (2) to calculate the impact strength.

$$I_s = \frac{E}{A} \quad (2)$$

where, $I_s$is the impact strength (J/m^2), E is absorbed energy (J), and A is cross-sectional area (m^2)

2.8 Hardness Test

The hardness test in this study uses the Vickers method. The aim is to measure the specimen's hardness. The test was conducted at the Mechanical Engineering Materials Testing Laboratory, Faculty of Engineering, Semarang State University, using the FM-800 Microhardness Tester. The specimen will be pressed using a pyramid-shaped diamond indenter with a square base at 136°. The pressure load is 5 gf, the holding time is 15 seconds, and the lens magnification is x50. Each variation was tested at three different points. The data obtained from the Vickers hardness test are the pressure load value, the diagonal values of traces 1 and 2, and the Vickers hardness value.

2.9 Microstructure

Microstructure was observed by taking microphotographs of each specimen to determine the tissue structure at the micronanoscale in composite materials [15]. Knowing the microstructure of a composite can help determine how its composition is characterized. Therefore, understanding the microstructure of composites is essential for estimating the mechanical strength to be tested. Microstructural photos were taken using a B-510 METROPTIKA ITALY microscope with a magnification of 50× in the Mechanical Engineering Laboratory, Faculty of Engineering, Semarang State University.

3. Results and Discussion

3.1 Specific Wear Rate

Wear tests are performed to determine the specimen's wear value. The tool used is the Ogoshi High Speed Universal Wear Testing Machine (OAT-U Type). The results of this test are the wear width values for the test specimen, which are then averaged. The testing was carried out three times for each composition variation in both the experimental and control groups to increase data accuracy. The test results are shown in Table 5. Figure 5 shows that the average specific wear rate varies across the different variations. The 10% CEFP variation has an average specific wear rate of 1.50×10^{-3} mm^3/kgm. The 20% CEFP variation has an average specific wear rate of 1.39×10^{-3} mm^3/kgm. The 30% CEFP variation has an average specific wear rate of 8.33×10^{-4} mm^3/kgm. Meanwhile, the control group has an average specific wear rate of 5.92×10^{-4} mm^3/kgm. The graph shows that the average specific wear rate of the experimental group decreased with increasing volume fraction of *Casuarina equisetifolia* fruit powder. The difference in the average specific wear rate between the experimental and control groups was 23.70%. Changes in the average specific wear rate showed a consistent downward trend. The average specific wear rate closest to the control group was the 30% CEFP specimen, which decreased by 28.93%. The decrease in the specific wear value in the experimental group may occur due to an increase in the volume fraction of *Casuarina equisetifolia* fruit powder. This is consistent with the findings of Sukrawan et al. [16], who reported that the higher the weight fraction of bamboo fibre, the lower the wear rate, resulting in a longer service life, better heat resistance, and increased hardness of the composite material. Similarly, the research by Kholil et al. [17] shows a decrease in wear with increasing lignin content in coconut fibre. In addition, the size of the powder used can affect the wear resistance of the composite material. As in the research of Nandiyanto et al. [18], which states that reducing the particle size of rice husks can reduce the wear rate and increase the friction coefficient of the composite material.

Table 5. Specific wear test results

Specimen code	Specific wear rate (mm^3/kgm)	Average specific wear rate (mm^3/kgm)
CEFP 10% 1	1.39×10^{-3}	1.50×10^{-3}
CEFP 10% 2	1.86×10^{-3}	
CEFP 10% 3	1.24×10^{-3}	
CEFP 20% 1	1.21×10^{-3}	1.39×10^{-3}
CEFP 20% 2	1.68×10^{-3}	
CEFP 20% 3	1.27×10^{-3}	
CEFP 30% 1	9.31×10^{-4}	8.33×10^{-4}
CEFP 30% 2	8.72×10^{-4}	
CEFP 30% 3	6.97×10^{-4}	
K 1	6.60×10^{-4}	5.92×10^{-4}
K 2	6.38×10^{-4}	
K 3	4.80×10^{-4}	

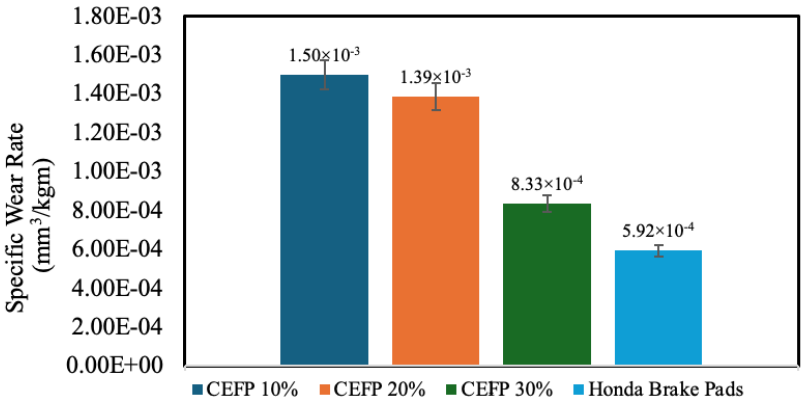

Figure 5. Average specific wear rate

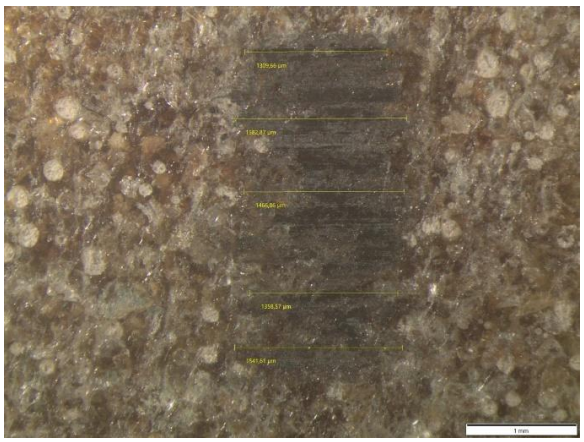

Figure 6. Wear width at 50× magnification

Figure 6 shows that the wear test resulted in surface erosion on the test specimen. This phenomenon occurs when the surface of the test specimen is scratched by a steel-based disc with a much higher hardness level than the test specimen, resulting in some material being removed from the surface [19]. Visually, the surface wear shows scratches with parallel grooves. The material displacement does not cause tearing. Based on this observation, the test specimen's surface undergoes abrasive wear [20]. The decrease in specific wear as the CEFP content increases shows that the filler helps the composite resist surface damage during sliding. When more CEFP is added, the surface becomes more resistant to scratching and material loss. The presence of Al_2O_3 particles also helps strengthen the surface because ceramic particles are harder than the epoxy matrix. However, this explanation is still based only on wear values and visual observation. It is not yet clear whether the improvement is caused by better particle bonding, better particle distribution, or reduced voids. To better understand the wear mechanism, future studies should examine the worn surface at higher magnification. This will help identify microcracks, particle pull-out, and interfacial failure that cannot be clearly observed under optical microscopy.

3.2 Impact Test

The tool used is the Gotech Impact Testing Machine, with a pendulum speed of 3.46 m/s, an α angle of 150°, and a span length of 64 mm. The energy given to the test piece is 25 J. Each variation is tested three times. The result obtained from this test is the value of the energy absorbed by the specimen. Then, to obtain the impact strength, the data are entered into equation 2, and the average of the resulting values is taken. The test results are shown in Table 6.

Table 6. Impact strength results

Specimen code	Absorbed energy (J)	Impact strength (J/mm^2)	Average impact strength (J/mm^2)
CEFP 10% 1	0.04	1.25×10^{-3}	1.15×10^{-3}
CEFP 10% 2	0.05	1.56×10^{-3}	
CEFP 10% 3	0.02	6.25×10^{-4}	
CEFP 20% 1	0.05	1.49×10^{-3}	1.90×10^{-3}
CEFP 20% 2	0.07	2.08×10^{-3}	
CEFP 20% 3	0.07	2.13×10^{-3}	
CEFP 30% 1	0.07	2.19×10^{-3}	2.08×10^{-3}
CEFP 30% 2	0.08	2.50×10^{-3}	
CEFP 30% 3	0.05	1.56×10^{-3}	
K 1	0.08	2.56×10^{-3}	2.50×10^{-3}
K 2	0.07	2.39×10^{-3}	
K 3	0.08	2.53×10^{-3}	

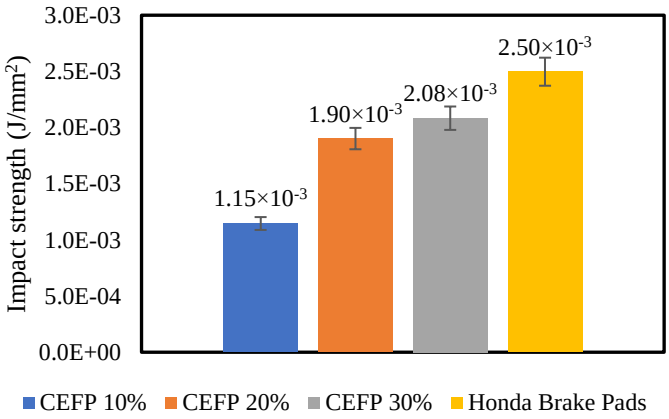

Figure 7. Average impact strength

Figure 7 shows that the average impact strength varies across the different variations. The 10% CEFP variation has an average impact strength of 1.15×10^{-3} J/mm^2. The 20% CEFP variation has an average impact strength of 1.90×10^{-3} J/mm^2. The 30% CEFP variation has an average impact strength of 2.08×10^{-3} J/mm^2. Meanwhile, the control group has an average impact strength of 2.50×10^{-3} J/mm^2. The graph shows that the average impact strength of the experimental group increased with increasing volume fraction of *Casuarina equisetifolia* fruit powder. The difference in the average impact strength of the experimental group was 37.35%. Changes in the average impact strength showed a consistent upward trend. The impact strength closest to the control group was the 30% CEFP specimen, which decreased by 20.19%. An increase in the impact strength in the experimental group may occur due to an increase in the number of volume fractions of the *Casuarina equisetifolia* fruit powder. It is in line with Fuad and Yudiono's [21] that more aegle marmelos shell particles can increase the impact strength, hardness, and wear resistance of composite materials. In the study, Wang et al. [22] observed the same trend: the greater the amount of corn straw fiber mixture added, the greater the composite material's impact strength. In addition, Liu et al. [23] state that the rough surface of natural fibers can provide good mechanical interlock between the fibres and the composite matrix, thereby improving energy absorption.

Figure 8 shows that the impact test conducted resulted in deformation in the form of a fault. During the impact testing, the test object breaks into two parts. After visual observation, the fault results indicate that the fracture in the test specimen is granular. It is characterized by pieces that can be reattached. The fractured surface is shiny when exposed to light. As well as on the observation of the fault surface, there are crystalline granules. The increase in impact strength with higher CEFP content shows that the composite can absorb more energy before breaking. This may happen because the particles help spread the stress more evenly inside the material. The fracture surface shows brittle behaviour, but the higher impact value at 30% CEFP suggests that the particles help slow down crack growth. Even so, the current explanation is still general. The real fracture mechanism, whether caused by particle breakage, matrix cracking, or weak bonding, cannot be

clearly seen from visual observation alone. A more detailed fracture surface analysis is needed to understand better how the particles improve energy absorption.

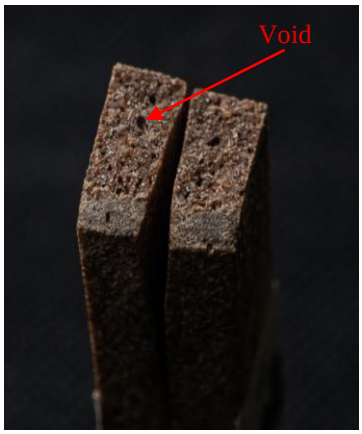

Figure 8. Fracture shape

3.3 Hardness Test

Hardness tests are performed to measure the hardness level of the specimen. The tool used is the Microhardness Tester Fm-800. The emphasis load value is 5 gf, the dwell time is 15 seconds, and the lens magnification is x50. Each variation is tested at three different points. The data obtained from the Vickers hardness test include the indentation load, the diagonals of indentations 1 and 2, and the Vickers hardness value. From the hardness value obtained, the average is taken. The test results are shown in Table 7.

Table 7. Hardness Vickers results

Specimen code	Test points	Hardness Vickers (HV)	Average hardness Vickers (HV)
CEFP 10%	1	7.1	7.4
	2	7.5	
	3	7.6	
CEFP 20%	1	9.1	9.2
	2	9.0	
	3	9.5	
CEFP 30%	1	13.7	13.4
	2	13.4	
	3	13.1	
K	1	17.2	18.23
	2	18.3	
	3	19.2	

Figure 9 shows that the average hardness varies across the different variations. The 10% CEFP variation has an average hardness of 7.4 HV. The 20% CEFP variation has an average hardness of 9.2 HV. The 30% CEFP variation has an average hardness of 13.4 HV. Meanwhile, the control group has an average hardness of 18.23 HV. The graph shows that the average hardness of the experimental group increased with increasing volume fraction of *Casuarina equisetifolia* fruit powder. The difference in the average hardness of the experimental group was 34.99%. Changes in the average hardness showed a consistent upward trend. The average hardness closest to the control group was the 30% CEFP specimen, which decreased by 36.04%. The increase in hardness in the experimental group may be due to a higher volume fraction of *Casuarina equisetifolia* fruit powder. This is in accordance with the research of Pujari and Srikiran [24], which shows that the hardness of composite materials increases with increasing volume fraction of palm kernel powder. Likewise, in the study by Akaluzia et al. [25], it was found that the greater the amount of hardwood charcoal powder used, the harder the composite materials become. In addition, the use of Al_2O_3 also affects the hardness value of resin matrix composites. Bazrgari et al. [26] reported that the addition of Al_2O_3 powder to resin matrix composites also increases the hardness. The hardness test results showed a correlation between the specific wear and hardness values: the higher the hardness, the lower the wear. This is consistent with the research by Ramanathan et al. [27], which found that higher hardness is associated with lower wear.

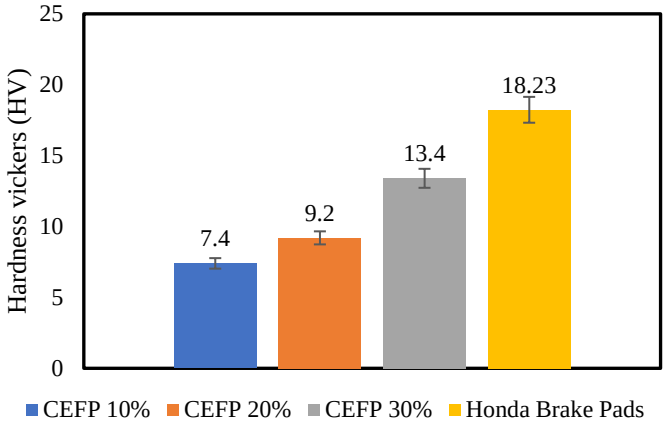

Figure 9. Average hardness Vickers

The increase in hardness with increasing CEFP content indicates that the filler enhances the composite's resistance to surface indentation. The particles reduce the mobility of the epoxy matrix, thereby strengthening the material under pressure. The addition of Al_2O_3 also contributes because it is a hard ceramic material. However, the hardness of the 30% CEFP specimen (13.4 HV) is still lower than that of the commercial pad (18.23 HV). This difference may be caused by uneven particle distribution, particle clumping, or weak bonding between the filler and the matrix. Therefore, further microstructural analysis is needed to clearly explain how the particles improve hardness and why the hardness value remains below the commercial standard.

3.4 Microstructure

Based on the observation of the microstructure, the addition of *Casuarina equisetifolia* fruit powder can cause changes in the microstructure of the composite. Figure 10(a) indicates that the most content is resin that is glossy and slightly dark in colour and looks empty in the absence of powder. This can happen because the composite contains 70% epoxy resin. In Figures 10(b-c), the blank part begins to be filled with *Casuarina equisetifolia* fruit powder. Microstructural observations revealed that the powder material composition in the experimental group was similar in color, making it difficult to distinguish. However, each material has distinct visual characteristics. *Casuarina equisetifolia* powder or natural fibre has a rough and uneven structure with irregular particles and small aggregates on its surface [28]. Meanwhile, Al_2O_3 powder has a smoother and rounder surface than natural powder [29].

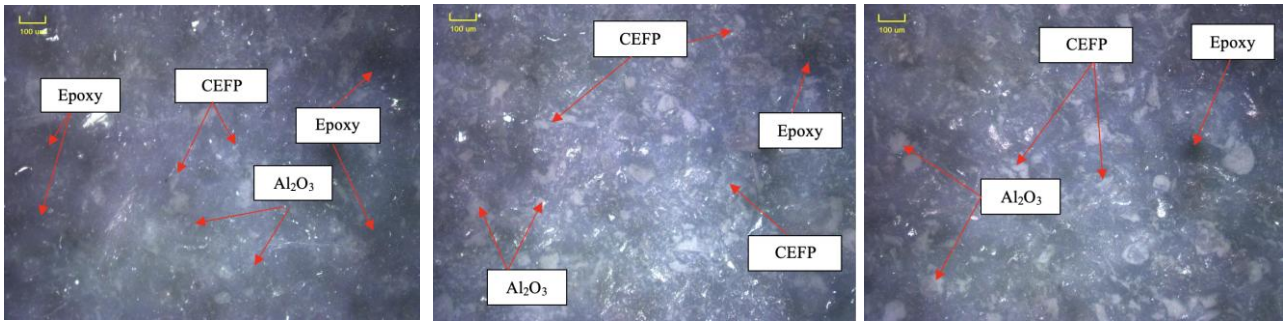

(a) CEFP 10% microstructure (b) CEFP 20% microstructure (c) CEFP 30% microstructure

Figure 10. Microstructures of CEFP at varying percentages: (a) 10%, (b) 20%, and (c) 30%

Figure 11 shows a different image from the others. The image shows copper (Cu) powder measuring approximately 200 µm in size. This can be identified through the physical characteristics of the Cu powder. According to Ding et al. [30] and Basheer et al. [31], the distribution of Cu powder particles tends to cluster, forming larger granules and a yellow powder. Microstructural observations of the control specimen revealed the presence of additional materials, some of which remain unidentified. Optical microscope images show that more CEFP particles are present in the composite as the filler percentage increases. This supports the improvement seen in wear, impact, and hardness tests. However, the 50× magnification only shows the general distribution of particles. It cannot clearly show small voids, interfacial bonding quality, or particle agglomeration. To better understand the relationship between microstructure and mechanical properties, future research should use SEM-EDX analysis. SEM can provide detailed images of particle distribution, particle-matrix bonding, and small cracks or voids. EDX can identify the elemental distribution inside the composite. This deeper analysis will help explain why higher CEFP content improves mechanical properties and how the composite structure can be further optimized.

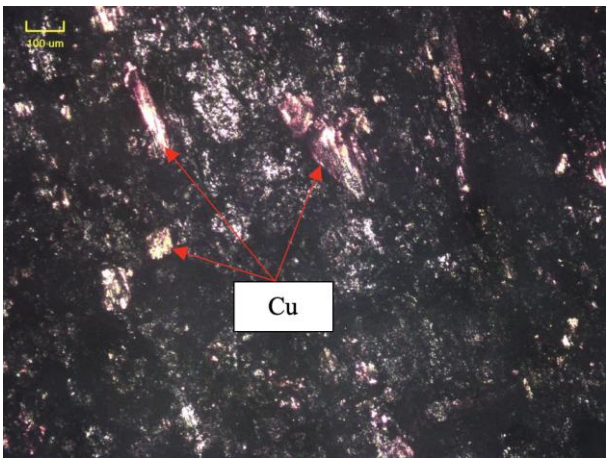

Figure 11. Honda brake pads microstructure

3.5 Comparison of Test Results of Experimental Group and Control Group

The results of the specific wear, impact strength, and composite hardness tests on the experimental groups showed increases in wear resistance, impact strength, and composite hardness. However, when compared, the control group's test results showed better wear resistance, impact strength, and hardness than those of the experimental group. This could be due to differences in the materials used. Microstructural observations revealed that Honda brake pads use Cu metal. Compared with *Casuarina equisetifolia* fruit powder, Cu material has a higher hardness. This is evident from the hardness test results, which showed that the control group's hardness was higher than that of the experimental group. Higher hardness can affect material wear, as Archard's law states that hardness is inversely proportional to wear [32]. This law is widely used in tribology experiments to measure the wear rate of materials [33]. This is consistent with the findings of Günay et al. [34], who showed that the lower the hardness of abrasive materials, the higher the wear, thereby reducing the wear resistance of composite materials. Voids formed during the manufacturing process can lead to material failure because the interfacial bonding between *Casuarina equisetifolia* fruit powder and the matrix is imperfect, thereby affecting the mechanical strength of the composite (wear resistance, energy absorption, and hardness) [35]. In the study, Durowaye et al. [36] said that the decrease in the mechanical strength (tensile strength, hardness, impact strength) of composites is caused by poor interface bonding or surface adhesion (between the filler and the matrix), as well as poor stress transfer between the particle interface and the matrix. Kannan et al. [37] reported that composite failure (decreased tensile strength, bending, and impact) occurs due to weak bonds between the matrix and fibers, particle clumping, and voids in the composites.

Another factor can be powder settling. This phenomenon can occur during the waiting process before compaction in the experimental group [38]. If the filler density is higher than that of the matrix, the filler will settle to the bottom of the composite surface. Conversely, if the filler density is lower than the matrix, the filler will rise to the surface [39]. The low density of the *Casuarina equisetifolia* fruit powder and the high density of the aluminum oxide powder compared to the epoxy resin cause the *Casuarina equisetifolia* fruit powder to rise to the surface. In contrast, the aluminum oxide settles at the bottom of the composite mixture. This is consistent with the research by Wang et al. [40], which showed that a longer settling time can reduce the mechanical strength of the composite. Furthermore, research by He et al. [39] showed a 10% decrease in the settling layer's wear value. Furthermore, the settling rate is influenced by the size of the powder used [41]. This condition can lead to uneven filler distribution [42]. Consequently, the test results in the experimental group were not superior to those in the control group.

4. Conclusions

Based on research, observation, and data analysis, it can be concluded that the addition of *Casuarina equisetifolia* fruit powder can affect the specific wear value, impact strength, and hardness of composite materials. The optimal composition of brake pads is 30% *Casuarina equisetifolia* fruit powder, 20% aluminum oxide powder, and 50% epoxy resin. The lowest average specific wear was observed for a volume fraction of 30% *Casuarina equisetifolia* fruit powder, with an average of 8.33×10^{-4} mm^3/kg. Meanwhile, the average specific wear of Honda brake pad specimens is 5.92×10^{-4} mm^3/kgm. The highest average impact strength was observed for a volume fraction of 30% *Casuarina equisetifolia* fruit powder, with a value of 2.08×10^{-3} J/mm^2. Meanwhile, the average impact strength of the Honda brake pad specimen is 2.50×10^-3 J/mm^2. The highest average hardness value was observed at a volume fraction of 30% *Casuarina equisetifolia* fruit powder, with a value of 13.4 HV. Meanwhile, the average hardness value of Honda brake pad specimens is 18.23 HV.

The results indicate that the 30% CEFP variation provides the best combination of mechanical properties among the variations tested. Its specific wear and impact strength values are close to those of Honda brake pads, while its hardness is higher than that of other variations, though it cannot match Honda's. So that the composite material studied has the potential to serve as an alternative for motorcycle brake pad composites. The current optical microscopy at 50× magnification serves as a preliminary survey of macro-dispersion. However, to fully resolve particle-matrix interface bonding and sub-micron porosity, future work must employ SEM-EDX (Scanning Electron Microscopy) to visualize the

nanoscale chemical distribution and structural integrity of the composite. Some suggestions for further research include optimizing the specimen manufacturing process to eliminate bubbles formed during material mixing (e.g., vacuum mixing or increasing the compaction pressure) and pre-treating the pinecone powder with a silane coupling agent or an alkali. In addition, vary the powder size used, incorporate temperature and time variations during sintering, apply pressure variations during compression, and add natural fibres and other metal materials to enhance the mechanical and physical properties of the composite constituent materials. Then perform tests on other mechanical and physical properties, such as friction coefficient, compressive strength, tensile strength, density, porosity, etc.

Acknowledgements
The authors thank the Department of Mechanical Engineering, Faculty of Engineering, Universitas Negeri Semarang, Central Java, Indonesia, for providing the laboratory facilities that enabled this work.

Funding
This study was not supported by any grants from funding bodies in the public, private, or not-for-profit sectors.

Declaration of Competing Interest
The author declares no conflicts of interest.

CRediT Authorship Contribution Statement
Nurin Tammima (Writing-original draft; Writing-review & editing; Data curation; Resources; Project administration)
Heri Yudiono (Validation; Formal analysis; Data curation; Supervision)
Muhammad Irfan Rifaldi (Data curation; Visualisation; Writing-review & editing)

Availability of Data and Materials
The data supporting this study's findings are available on request from the corresponding author.

Ethics Declarations
This study did not involve human participants or animals. Ethical approval was therefore not required.

Generative Artificial Intelligence Declarations
The authors stated that generative AI was not used to generate content, ideas, or theories. We have just utilised AI to enhance readability and refine the language. This was used with extreme human control and oversight. The authors take full responsibility for reviewing and approving the content.

References
[1] A. G. Joshi, K. N. Bharath, and S. Basavarajappa, "Recent progress in the research on natural composite brake pads: a comprehensive review," *Tribology - Materials, Surfaces & Interfaces*, vol. 17, no. 3, pp. 237–259, 2023.
[2] B. Mylsamy, V. Chinnasamy, S. K. Palaniappan, S. P. Subramani, and C. Gopalsamy, "Effect of surface treatment on the tribological properties of Coccinia Indica cellulosic fiber reinforced polymer composites," *Journal of Materials Research and Technology*, vol. 9, no. 6, pp. 16423–16434, 2020.
[3] B. Praveenkumar and S. D. Gnanaraj, "Case studies on the applications of phenolic resin-based composite materials for developing eco-friendly brake pads," *Journal of The Institution of Engineers (India): Series D*, vol. 101, no. 2, pp. 327–334, 2020.
[4] E. K. Radwan, R. A. Omar, and A. Marey, "Upcycling of easy separated Casuarina Equisetifolia fruit waste as a biosorbent: Tailoring the surface modification to enhance selective removal of cationic dye or simultaneously removal of cationic and anionic dyes," *Applied Water Science*, vol. 13, no. 10, pp. 1–17, 2023.
[5] S. Tiwari and S. Talreja, "A critical overview on Casuarina Equisetifolia," *Pharmacognosy Reviews*, vol. 17, no. 34, pp. 255–261, 2023.
[6] A. Osman, A. Elhakeem, S. Kaytbay, and A. Ahmed, "A comprehensive review on the thermal, electrical, and mechanical properties of graphene-based multi-functional epoxy composites," *Advanced Composites and Hybrid Materials*, vol. 5, no. 2, 2022.
[7] D. Huo, X. Li, B. Yuan, and D. Nan, "Enhancing mechanical properties of epoxy resin composites with aluminum oxide-modified graphene oxide," *Diamond and Related Materials*, vol. 151, p. 111864, 2025.
[8] P. Ravichandran, P. Sugumaran, S. Seshadri, and A. H. Basta, "Optimizing the route for production of activated carbon from Casuarina Equisetifolia fruit waste," Royal Society Open Science, vol. 5, no. 7, pp. 1–12, 2018.
[9] N. Arif and S. Ahmad, "A review on the synthesis, properties, applications, and harmful effects of alumina," *International Journal of Trend in Scientific Research and Development*, vol. 6, no. 3, pp. 1586–1594, 2022.
[10] A. P. Irawan, D. F. Fitriyana, J. P. Siregar, T. Cionita, P. T. Anggarina, D. W. Utama, et al., "Influence of varying concentrations of epoxy, rice husk, Al_2O_3, and Fe_2O_3 on the properties of brake friction materials prepared using hand layup method," *Polymers*, vol. 15, p. 2597, 2023.
[11] H. Yudiono, J. P. Siregar, S. Asri, H. Hidayat, D. B. Chikam, J. A. Aprilian, et al., "Effect of alkalization time on the toughness and strength of jute sack waste lamina composite as an alternative car bumper material," *International Journal of Automotive and Mechanical Engineering*, vol. 21, no. 4, pp. 11809–11820, 2024.

[12] A. Adekunle, M. Okunlola, P. Omoniyi, A. Adeleke, P. Ikubanni, T. Popoola, et al., "Development and analysis of friction material for eco-friendly brake pad using seashell composite," *Scientia Iranica*, vol. 30, no. 5, pp. 1562–1571, 2023.
[13] M. Kwak, P. Robinson, A. Bismarck, and R. Wise, "Microwave curing of carbon-epoxy composites: Penetration depth and material characterisation," *Composites Part A: Applied Science and Manufacturing*, vol. 75, pp. 18–27, 2015.
[14] ISO, ISO 179-1 Plastics-Determination of Charpy impact properties, 2023.
[15] S. Gao, R. Wang, Y. Xu, H. Zhang, S. Zhang, M. Xu, et al., "Facile construction of a micro-nano structure of green polyvinyl alcohol-based composite aerogel with superior mechanical properties, thermal insulation, and fire safety," *Polymer Degradation and Stability*, vol. 241, p. 111522, 2025.
[16] Y. Sukrawan, A. Hamdani, and S. A. Mardani, "Effect of bamboo weight faction on mechanical properties in non-asbestos composite of motorcycle brake pad," *Materials Physics and Mechanics*, vol. 42, pp. 367–372, 2019.
[17] A. Kholil, S. T. Dwiyati, R. Wirawan, and E. M, "Brake pad characteristics of natural fiber composites from coconut fibre and wood powder," *Journal of Physics: Conference Series*, vol. 2019, no. 1, p. 012068, 2021.
[18] A. B. D. Nandiyanto, S. N. Hofifah, G. C. S. Girsang, S. R. Putri, B. A. Budiman, F. Triawan, and et al., "The effects of rice husk particles size as a reinforcement component on resin-based brake pad performance: from literature review on the use of agricultural waste as a reinforcement material, chemical polymerization reaction of epoxy resin, to experiments," *Automotive Experiences*, vol. 4, no. 2, pp. 68–82, 2021.
[19] B. Wang, H. Chu, C. Song, Q. Zhang, and H. Zhang, "Characteristics and mechanism of diamond abrasive grains wear under NMQL-assisted grinding of SiCf/SiC composites," *Diamond and Related Materials*, vol. 158, p. 112616, 2025.
[20] W. Li, X. Hu, G. Long, A. Shang, and B. Guo, "Grain wear properties and grinding performance of porous diamond grinding wheels," *Wear*, vol. 530, p. 204993, 2023.
[21] M. T. N. Fuad and H. Yudiono, "The effect of Aegle Marmelos shell particles volume fraction on hardness, toughness, and wear rate of epoxy matrix composites as motorcycle brake pads," *Journal of Mechanical Engineering and Sciences*, vol. 17, no. 1, pp. 9338–9348, 2023.
[22] Z. Y. Wang, J. Wang, and Y. H. Ma, "The evaluation of physicomechanical and tribological properties of corn straw fibre reinforced environment-friendly friction composites," *Advances in Materials Science and Engineering*, vol. 2019, Art. no. 1562363, 2019.
[23] Y. Liu, X. Lv, J. Bao, J. Xie, X. Tang, J. Che, et al., "Characterization of silane treated and untreated natural cellulosic fibre from corn stalk waste as potential reinforcement in polymer composites," *Carbohydrate Polymers*, vol. 218, pp. 179–187, 2019.
[24] S. Pujari and S. Srikiran, "Experimental investigations on wear properties of palm kernel reinforced composites for brake pad applications," *Defence Technology*, vol. 15, no. 3, pp. 295–299, 2019.
[25] R. O. Akaluzia, F. O. Edoziuno, A. A. Adediran, B. U. Odoni, S. Edibo, and T. M. A. Olayanju, "Evaluation of the effect of reinforcement particle sizes on the impact and hardness properties of hardwood charcoal particulate-polyester resin composites," *Materials Today: Proceedings*, pp. 570–577, 2020.
[26] D. Bazrgari, F. Moztarzadeh, A. A. Sabbagh-Alvani, M. Rasoulianboroujeni, M. Tahriri, and L. Tayebi, "Mechanical properties and tribological performance of epoxy/Al_2O_3 nanocomposite," *Ceramics International*, vol. 44, pp. 1220–1224, 2018.
[27] K. Ramanathan, P. Saravanakumar, S. Ramkumar, P. P. Kumar, and S. R. Surender, "Development of asbestos-free brake pads: Using lemon peel powder," *International Journal of Innovative Research in Science, Engineering and Technology*, vol. 6, no. 3, pp. 4449–4455, 2017.
[28] J. Wang, S. Yang, X. Wang, L. Zhang, and Y. Zhao, "Comparative efficacy of natural seed coats in regulating protein aggregation in pre-roasted pine kernels and enhancing associated techno-functionality," *Food Chemistry*, vol. 479, p. 143766, 2025.
[29] Z. Y. Luo, W. Han, X. J. Yu, W. Q. Ao, and K. Q. Liu, "In-situ reaction bonding to obtain porous SiC membrane supports with excellent mechanical and permeable performance," *Ceramics International*, vol. 45, pp. 9007–9016, 2019.
[30] S. Ding, X. Wu, C. Chen, M. Gui, P. Sun, F. Yang, et al., "Enhanced adhesion strength of copper deposited epoxy composite films for chip substrates by tuning copper oxide and internal stress," *Applied Surface Science*, vol. 684, p. 161911, 2025.
[31] B. Basheer, M. G. Akhil, T. P. D. Rajan, P. Agarwal, and V. Vijay Saikrishna, "Copper metallization of carbon fiber-reinforced epoxy polymer composites by surface activation and electrodeposition," *Surface and Coatings Technology*, p. 131016, 2024.
[32] E. Rabinowicz, "The wear coefficien-magnitude, scatter, use," *Journal of Lubrication Technology*, vol. 103, pp. 188–193, 1981.
[33] J. Hu, H. Song, S. Sandfeld, X. Liu, and Y. Wei, "Breakdown of Archard law due to transition of wear mechanism from plasticity to fracture," *Tribology International*, vol. 173, p. 107660, 2022.
[34] M. Günay, M. E. Korkmaz, and R. Özmen, "An investigation on braking systems used in railway vehicles," *Engineering Science and Technology, an International Journal*, vol. 23, no. 2, pp. 421–431, 2020.

[35] N. Siddgonde, V. Kaushik, and A. Ghosh, "Experimental and numerical characterization of E-glass / epoxy plain woven fabric composites containing void defects," *Aerospace Science and Technology*, vol. 155, Part 3, p. 109731, 2024.
[36] S. Durowaye, G. Lawal, O. Sekunowo, and A. Onwuegbuchulem, "Synthesis and characterization of hybrid polypropylene matrix composites reinforced with carbonized Terminalia Catappa shell particles and Turritela Communis shell particles," *Journal of Taibah University for Science*, vol. 12, no. 1, pp. 79–86, 2018.
[37] G. Kannan, R. Thangaraju, P. Kayaroganam, and J. P. Davim, "The combined effect of banana fiber and fly ash reinforcements on the mechanical behavior of polyester composites," *Journal of Natural Fibers*, vol. 19, no. 15, pp. 11384–11403, 2022.
[38] S. Samal, "Effect of shape and size of filler particle on the aggregation and sedimentation behavior of the polymer composite," *Powder Technology*, pp. 43–51, 2020.
[39] H. He, G. Fan, F. Saba, Z. Tan, Z. Su, D. Xiong, et al., "Enhanced distribution and mechanical properties of high content nanoparticles reinforced metal matrix composite prepared by flake dispersion," *Composites Part B: Engineering*, vol. 252, p. 110514, 2023.
[40] J. Wang, R. Yang, S. Sun, and T. Lv, "Multi-scale microstructural evolution and mechanical property response in needled ceramic matrix composites: Effect of deposition time variation," *Materials Today Sustainability*, p. 101296, 2025.
[41] S. Yano, Y. I. Hsu, and H. Uyama, "Improvement of mechanical and thermal properties of epoxy composites with citric acid modified and defibrated cellulose filler," *Polymer Degradation and Stability*, p. 111482, 2025.
[42] K. W. Abesho, M. G. Jiru, H. G. Lemu, and M. A. Alfeki, "Study of mechanical and physical properties of pineapple leaf fiber and coffee husk filler reinforced polymer composite using response surface method," *Polymer Testing*, p. 108915, 2025.